

IMPROVEMENT OF CORROSION RESISTANT COATING FOR SILICON-CARBIDE FUEL CLADDING IN OXYGENATED HIGH TEMPERATURE WATER

R. ISHIBASHI, S. TANABE, T. KONDO

Hitachi-GE Nuclear Energy, Ltd.

3-1-1, Saiwai-cho, Hitachi, Ibaraki-ken 317-0073, Japan

S. YAMASHITA, T. FUKAHORI

Nuclear Science Research Institute, Japan Atomic Energy Agency

2-4, Shirakata, Tokai-mura, Naka-gun, Ibaraki-ken 319-1195, Japan

ABSTRACT

To improve the corrosion resistance of silicon carbide (SiC) in boiling water reactor (BWR) environments, corrosion resistant coatings to SiC substrates and joint portions are being developed. One critical issue left for the practical application of SiC fuel cladding and a fuel channel box is hydrothermal corrosion. Corrosion behavior of candidate coatings to SiC substrates and joint portions were evaluated in unirradiated high purity water with a dissolved oxygen of 8.0 mg/l at temperatures of 561 K and 633 K for about 3.6 Ms. The SiC substrate lost 1.8 times more weight at 633 K than at 561 K. At both temperatures, titanium coating protected SiC substrates and joint portions by the same mechanism of TiO₂ formation. The results indicate that Ti coating applied on SiC substrates and joint portions is potentially effective as an environment barrier coating in oxygenated high temperature water.

1. Introduction

In light of the lessons learned in the aftermath of the Fukushima Daiichi nuclear accident, we have been developing various technologies for light water reactors (LWRs) with an emphasis on safety. The Ministry of Economy, Trade and Industry (METI) of Japan has been sponsoring and organizing a program to create the technical basis for practically using accident-tolerant fuels (ATFs) and other accident-tolerant components in LWRs.¹ Various alternative materials for fuel cladding and core structures of LWRs have been considered, and SiC-based materials—particularly SiC-fiber-reinforced SiC-matrix ceramic composites (SiC/SiC composites)—are thought to provide outstanding passive safety features in “beyond-design-basis severe-accident scenarios.”^{2,3} Replacement of conventional Zircaloy fuel cladding with silicon carbide (SiC) fuel cladding (which has a lower hydrogen-generation rate and lower heat

of reaction) is expected to significantly decrease the amount of hydrogen generated from fuel claddings during severe accidents.³ Thus, manufacturing and integration technology, such as end-plug technology, is being developed to resolve certain issues.^{4,5,6}

However, there are many critical issues with the practical application of SiC fuel cladding, one of which is hydrothermal corrosion. Hydrothermal corrosion can cause immediate critical issues as well as swelling-induced cracking and fuel-temperature issues.⁴ In hydrothermal light water reactor (LWR) coolant environments, the silicon in SiC undergoes oxidation and produces silica that readily dissolves in water. In fuel-cladding applications, depending on the in-pile recession kinetics of SiC, loss of cladding thickness can potentially expose the fiber-matrix interface and allow the silica concentration in the coolant to build up to the point of saturation, beyond which silica can deposit in the cold regions of the power loop.⁷ The amount of dissolved silica from SiC is likely to be larger in the coolant of a boiling water reactor (BWR) with higher dissolved oxygen activity than in the coolant of a pressurized water reactor (PWR) because the dissolved oxygen activity in water can greatly increase SiC recession.⁷ The dissolved oxygen concentration (DO) in the inlet water of actual BWRs is generally controlled at a low level, e.g., less than 200 $\mu\text{g/l}$ for a BWR-normal water chemistry (NWC) environment. However, some oxidants, such as oxygen and hydrogen peroxide, are generated by radiolysis and promote the oxidation of SiC in actual reactors. Silica concentration in the coolant of BWRs should be kept low because silica deposited on turbine vanes might decrease efficiency. Therefore, silica dissolution from SiC fuel cladding in BWRs needs to be suppressed.

Corrosion-resistant coatings and technology for decreasing the recession rate of SiC are being developed.⁸⁻¹² Sintering additives and the crystalline orientation of SiC affect corrosion behavior in high-temperature water.^{8,9} Silicon carbide formed by chemical vapor deposition (CVD-SiC) is expected to have a lower recession rate than SiC formed in other ways because of its high purity due to the absence of sintering additives. Corrosion-resistant coatings made using industrial technologies, such as electrolytic deposition, physical vapor deposition (PVD), and vacuum plasma spraying have been examined.¹⁰⁻¹² Metals (such as Cr^{11,12} and Ti¹²), alloys (such as Zircaloy-2^{11,12}), and metal nitrides (such as CrN¹¹ and TiN¹¹) have also been coated onto SiC as a surface layer. During the hydrothermal corrosion testing for 3.6 Ms, both Cr and Ti coatings protect the CVD-SiC substrate, which at 561 K dissolves in pure water with a DO of 8.0 mg/l, whereas the Zr coating significantly disbonded¹².

Furthermore, environment barrier coating on joint portions is necessary to protect joint materials with low corrosion resistance in reactor coolant. Although candidate joint materials such as sintered SiC, and mixture of Al-Si-O-C oxide and metal using air brazing process show little obvious microstructural change by irradiation,¹³ it is necessary to be careful about their corrosion in reactor coolant since sintered SiC is predicted to be less corrosion resistant

than CVD-SiC because of additives and since alumina and silica are dissolved in high temperature water^{14,15}. Thus, we are developing Ti spray coating on joint portions¹⁶.

The objective of this study was to clarify the feasibility of corrosion-resistant coatings on SiC substrates and joints in BWR coolant environments by evaluating the corrosion resistance of Cr and Ti coatings in oxygenated pure water at high temperatures under unirradiated conditions.

2. Experimental Procedures

2.1 Materials and Coating

Configurations of specimens are listed in Table 1. Two types of coated specimens without or with joint portions (hereinafter called substrate specimens and joint specimens, respectively) were prepared. Base specimens were overcoated liquid-phase-sintered (LPS)-SiC/SiC composite plates (40.0×9.8×1.0 (mm) or 19.9×9.8×1.0 (mm)) with high-purity CVD-SiC. The CVD-SiC coating was processed to be 90–120 μm thick by using thermal CVD by ADMAP Inc. Then coatings consisting of Cr or Ti were formed on the overcoated surfaces of the base specimens by PVD processing and subsequent heat treatment. Base specimens were rotated in argon gas while the metal coatings were deposited using the unbalanced magnetron sputtering method with a bias voltage of 150 V. The coatings were layered up to 10–20 μm thick by deposition from sputtering targets of pure Cr or pure Ti after a Cr bonding layer had been applied to the CVD-SiC substrate. The Cr-coated specimens and the Ti-coated specimens were heat-treated at 1223 K for 1.8 ks (1 ks = 10³ s). The butt joint specimens were brazed with Si by using a graphite heating element for heating to 1723 K at a heating rate of 0.83 K/s in argon gas atmosphere. The same Ti coating as the substrate specimen was processed on surface of the joint specimens 10 mm long from each end by masking the joint portions. Then, the joint portions were covered with Ti coating about 200 μm thick by vacuum plasma spraying. The sprayed Ti coating 20 mm long has an overlap about 5 mm with the Ti coating from each end.

Table 1 Configurations of coated specimens without or with joint.

Specimen	Base		Coating	
	Substrate	Joining	Substrate	Joint portion
Substrate (without joint)	CVD-SiC overcoated SiC/SiC composite [40.2×10.0×1.2(mm)]	-	Cr or Ti coating using PVD and subsequently heat treatment [all surface]	-
Joint	2 pieces of CVD-SiC overcoated SiC/SiC composite [20.1×10.0×1.2(mm)]	Butt joining by Si brazing	Ti coating by PVD and subsequently heat treatment [10 mm long from each end]	Ti coating by vacuum plasma spraying [20 mm long]

2.2 Hydrothermal Corrosion Test

The test apparatus consisted of an autoclave and circulation loop for high-purity water at high temperature. Water was controlled at an electric conductivity less than 0.010 mS/m and a DO 8.0 mg/l in a water-chemistry-regulation tank. The water was let into a test chamber after being pressurized and heated to 561±5 K at 7.9 MPa or 633±5 K at 20.2 MPa. The DO of 8.0 mg/l is intended to simulate a high oxidant concentration produced by water radiolysis. The temperature of 561 K corresponds to that of BWR coolant, whereas the test at 633 K was intended to accelerate corrosion phenomena. Three specimens for each coating were tested under the same conditions. The specimens were balanced and observed after time lapses of 0.72, 1.8, and about 3.6 Ms (1 Ms = 10⁶ s).

2.3 Analysis of Coatings

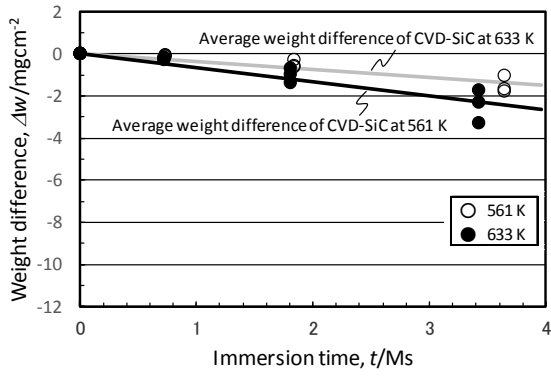
The coatings before and after hydrothermal corrosion testing were evaluated by weighing then by X-ray diffraction (XRD) analysis to identify their constituent phases, external observation, and scanning electron microscopy (SEM). The XRD profiles were measured by using the $\theta/2\theta$ method using copper $K\alpha$ ($\lambda:1.5418 \text{ \AA}$) and analyzed by using standard data of the International Centre for Diffraction Data (ICDD). Top views and cross-sectional images of the coatings were observed through SEM. The base specimens and the Ti-coated joint specimens for cross-sectional observation were finished by argon ion milling. Cross-sectional specimens from the Cr-coated and Ti-coated specimens were prepared by focused ion beam milling after W deposition. Oxidation of the coatings was evaluated by cross-sectional line analysis using SEM energy-dispersive X-ray spectroscopy (EDX) and Auger electron spectroscopy (AES).

3. Results

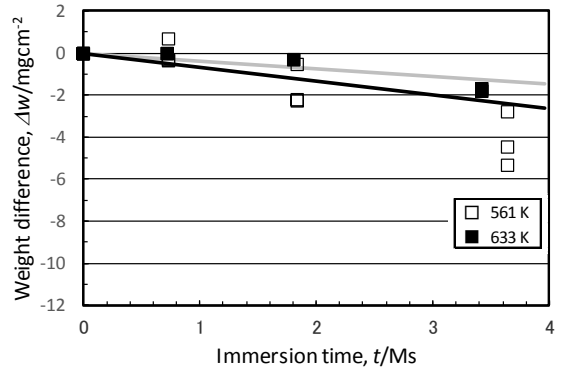
The weight differences determined by weighing the base specimens and the coated specimens before and after hydrothermal corrosion testing are shown in Fig. 1. Hydrothermal corrosion tests at 633 K resulted in larger weight differences than did tests at 561 K for the base specimens (CVD-SiC surface) as shown in Fig. 1(a). Gray and black solid lines are regression lines for weight differences of the base specimens at 561 K and 633 K, respectively. The Cr-coated substrate specimens lost weight after 1.8 Ms, whereas the Ti-coated substrate specimens changed little in weight at either temperature. The Ti-coated joint specimens slightly gained weight and changed little in weight after 0.72 Ms, although the specimens, whose sprayed coating was delaminated at the edges, lost weight as shown in Fig. 1(d). The Ti-coated substrate specimens and the Ti-coated joint specimens at showed no significant distinction in weight difference 561 K or 633 K.

The appearances of specimens before and after hydrothermal corrosion testing are shown in Fig. 2. Surface discoloration and disbondment of coating were observed. The discoloration of each surface and disbondment occurred at the edges of some specimens and expanded to the main surfaces of the Cr-coated specimens. The disbondment corresponds to the weight losses plotted in Fig. 1.

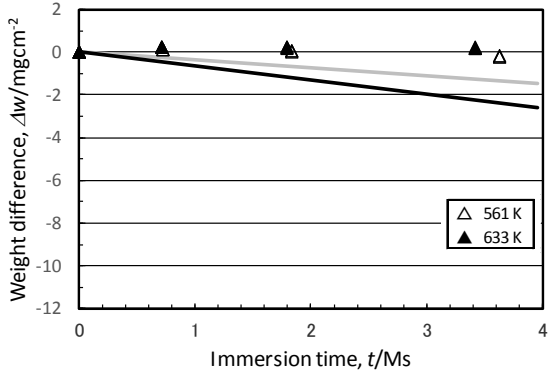
Secondary electron images of the coatings before and after hydrothermal corrosion testing are shown in Fig. 3. Regions of corrosion products in cross-section images were identified as higher-oxygen-concentration regions by line analyses using SEM-EDX and AES, and corrosion products were identified using XRD. For the base specimens (CVD-SiC surface), dissolution of SiC was observed after testing. The CVD-SiC surface tested at 633 K was partially covered with deposits of CrOOH. For the Cr-coated substrate specimens, corrosion products of Cr₂O₃ and CrOOH were identified by XRD, and oxidation penetrated the coating after hydrothermal corrosion testing. For the Ti-coated substrate specimens after hydrothermal corrosion testing, oxidation was limited to the coating surface, and granular corrosion products were observed. No significant change in oxidation behavior was observed between 561 K and 633 K. Pores are observed in the coating, which were probably generated by a reaction between contaminants and carbon diffused from SiC substrate during the coating process. For the Ti-coated joint specimens after hydrothermal corrosion testing, no corrosion of braze material under the sprayed coating was observed in the specimens without coating delamination. Observed cracking in cross-sectional SEM images was generated during the cutting process after the testing. Corrosion product of TiO₂ was observed in both the Ti-coated substrate and joint specimens after the hydrothermal corrosion tests.



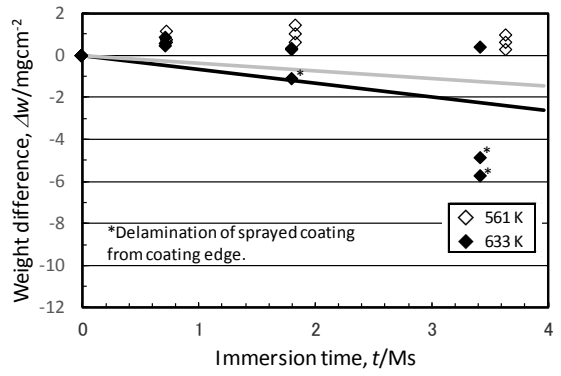
(a) Base (Substrate)



(b) Cr-coated (Substrate)



(c) Ti-coated (Substrate)



(d) Ti-coated (Joint)

Fig. 1 Weight difference of base and coated specimens between before and after hydrothermal corrosion tests.

(Gray and black lines are regression lines for weight differences of the base specimens at 561 K and 633 K, respectively.)

	Before test	After 3.6 Ms at 561 K	After 3.4 Ms at 633 K
Base (Substrate) 10 mm			
Cr-coated (Substrate)			
Ti-coated (Substrate)			
Ti-coated (Joint)			

Fig. 2 Appearances of one specimen for each coating before and after hydrothermal corrosion test.

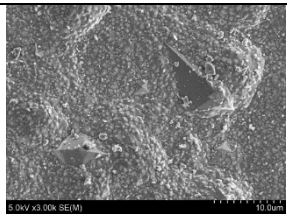
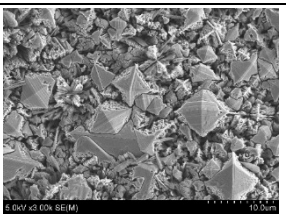
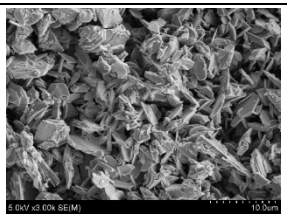
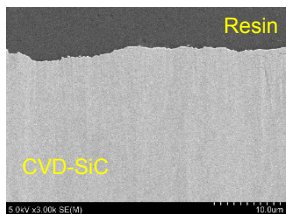
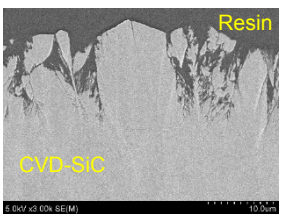
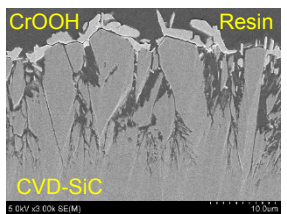
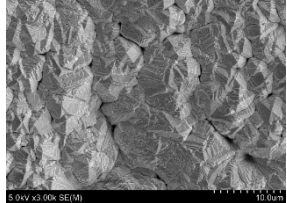
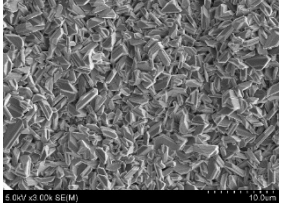
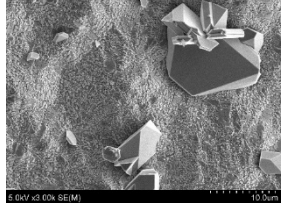
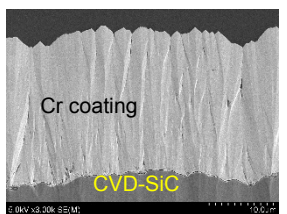
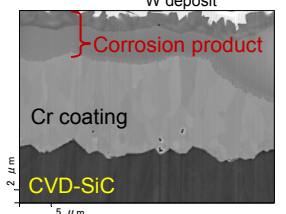
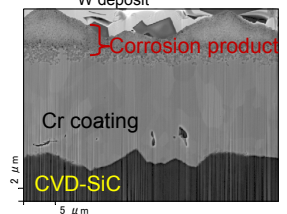
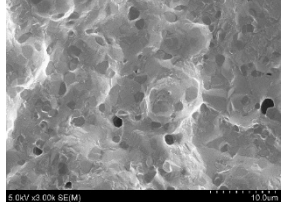
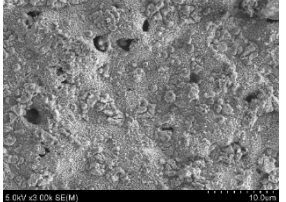
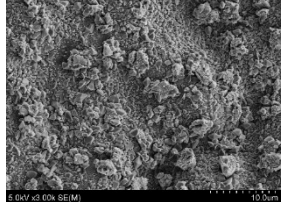
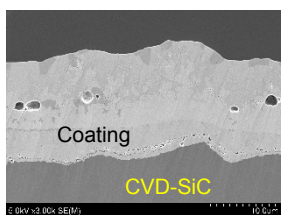
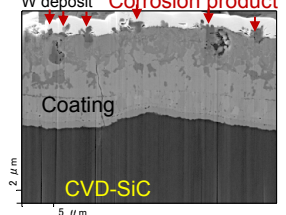
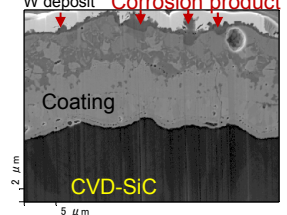
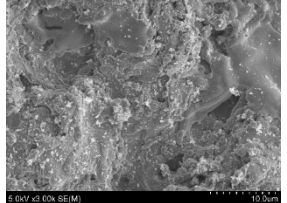
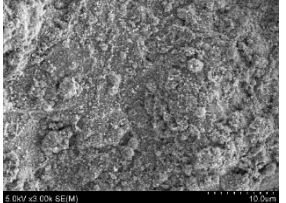
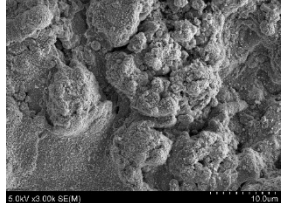
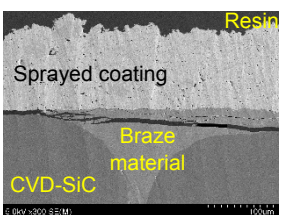
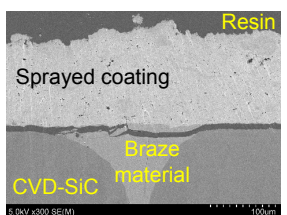
Specimen	View	Before test	After 3.6 Ms at 561 K	After 3.4 Ms at 633 K
Base (Substrate)	Top view			
	Cross section			
Cr-coated (Substrate)	Top view			
	Cross section			
Ti-coated (Substrate)	Top view			
	Cross section			
Ti-coated (Joint)	Top view			
	Cross section	No image		

Fig. 3 Secondary electron images of base and coated specimens before and after hydrothermal corrosion test.

4. Discussion

4.1 Dissolution of SiC

Corrosion rates of CVD-SiC overcoated specimens in oxygenated high temperature water are listed in Table 2. The SiC substrate lost 1.8 times more weight in water with a DO of 8 mg/l at 633 K than at 561 K. The ratio of 1.8 between temperatures at 561 and 633 K is much smaller than the ratio of 130 between DOs of 0.3 and 8.0 mg/l. The cross-sectional SEM images at the surface of the base specimens in Fig.3 reveal that CVD-SiC was dissolved in high temperature water. Deposits of CrOOH on CVD-SiC after the test at 633 K were formed from Cr ion in water during the hydrothermal corrosion test. The Cr ion in water was derived from Cr-containing alloys used in jigs, piping and a chamber at high temperature. It is uncertain how the deposits affected dissolution of SiC.

Table 2 Corrosion rates of CVD-SiC overcoated specimens in high temperature water

Specimens	Temperature (K)	Pressure (MPa)	DO (mg/l)	Flow rate (m/s)	Corrosion rate (mg/cm ² h ¹)	Ratio	Reference
CVD-SiC overcoated SiC-fiber-bonded Ceramics	561	8	0.3	2×10^{-4}	1.82×10^{-5}	1.0	Previous study ¹²⁾
	561	8	8.0	2.1×10^{-4}	2.31×10^{-3}	130	
CVD-SiC overcoated LPS-SiC/SiC composite	561	8	8.0	2.1×10^{-4}	1.33×10^{-3}	1.0	This study
	633	20	8.0	8.2×10^{-5}	2.38×10^{-3}	1.8	

4.2 Corrosion resistance of coatings

Titanium coating protected SiC substrates and joint portions in high temperature water with a DO of 8.0 mg/l at 561 K and 633 K. Oxidation penetrated the Ti coating much less than the Cr coating during the hydrothermal corrosion tests. It is considered that TiO₂ formed from the Ti function as a diffusion barrier and has low solubility in oxygenated pure water at 561 K and 633 K. The calculated solubility of TiO₂ is much less than those of SiO₂, Cr₂O₃, and CrOOH in pure water with a DO of 8.0 mg/l at 561 K.¹² Weight loss of Cr-coated substrate specimens is attributed to coating disbonding as well as Cr₂O₃ and CrOOH dissolving. It is considered that penetration of oxidation causes the Cr-coating to disbond. Sprayed Ti coating delaminated in some specimens. One reason for this is considered to be residual stress introduced by the thermal spraying process. Thus, a technique to control residual stress in the sprayed coatings needs to be developed to improve reliability of the coating for joint portions.

5. Conclusions

Corrosion behavior of candidate coatings to SiC substrates and joint portions were evaluated in unirradiated high purity water environments with a DO of 8.0 ppm at temperatures of 561 K and 633 K for about 3.6 Ms. The SiC substrate lost 1.8 times more weight at 633 K than at 561 K. Titanium coating protected SiC substrates and joint portions by the same mechanism of TiO₂ formation at both temperatures. The results indicate that Ti coating is potentially effective to protect SiC substrates and joint portions as an environment barrier coating in oxygenated high temperature water.

Acknowledgements

This study is the result of “Development of Technical Basis for Introducing Advanced Fuels Contributing to Safety Improvement of Current Light Water Reactors” carried out under the Project on Development of Technical Basis for Improving Nuclear Safety by the Ministry of Economy, Trade and Industry (METI) of Japan. We would like to express our gratitude to Dr. K. Ishida of Hitachi, Ltd. for discussing corrosion resistance of candidate coatings and joint materials.

Reference

- [1] S. YAMASHITA, F. NAGASE, M. KURATA, T. NOZAWA, S. WATANABE, K. KIRIMURA, K. KAKIUCHI, T. KONDO, K. SAKAMOTO, K. KUSAGAYA, S. UKAI, and A. KIMURA, “Technical Basis of Accident Tolerant Fuels Updated Under a Japanese R&D Project”, *Proc. WRFPM 2017*, Jeju Island, Korea, September 10-14, 2017, paper No. A176_F-176, Korean Nuclear Society (2017).
- [2] S. J. ZINKLE, K. A. TERRANI, J. C. GEHIN, L. J. OTT, and L. L. SNEAD, “Accident tolerant fuels for LWRs: A perspective,” *Journal of Nuclear Materials*, **448**, 1–3, 374–379, (2014).
- [3] R. ISHIBASHI, T. IKEGAWA, K. NOSHITA, K. KITOU, and M. KAMOSHIDA, “Hydrogen explosion prevention system using SiC fuel cladding for large scale BWRs with inherently safe technologies,” *Mechanical Engineer Journal*, **3**, paper No. 15-00215, (2016).
- [4] Y. KATOH, K. A. TERRANI, and L. L. SNEAD, Systematic Technology Evaluation Program for SiC/SiC Composite-based Accident-Tolerant LWR Fuel Cladding and Core Structures, ORNL/TM-2014/210, (2014).
- [5] Y. KATOH, L. L. SNEAD, T. CHENG, C. SHIH, W. D. LEWIS, T. KOYANAGI, T. HINOKI, C. H. HENAGER Jr., and M. FERRARIS, “Radiation-tolerant joining technologies for silicon carbide ceramics and composites,” *Journal of Nuclear Materials*, **448**, 1–3, 497–511, (2014).
- [6] R. ISHIBASHI, Y. TAKAMORI, X. ZHANG, T. KONDO, and K. MIYAZAKI, “Development of Joining Technology using Local Heating for SiC Fuel Cladding,” *Proc. Top Fuel 2016*,

- Boise, ID, September 11-15, 2016, paper No.17636, pp.805–813, American Nuclear Society (2016).
- [7] K. A. TERRANI, Y. YANG, Y. J. KIM, R. REBAK, H. M. MEYER, and T. J. GERCZAK, “Hydrothermal corrosion of SiC in LWR coolant environments in the absence of irradiation”, *Journal of Nuclear Materials*, **465**, 488–498 (2015).
- [8] Y. HYODO, Y. TSUCHIYA, S. KONDO, T. HINOKI, and F. KANO, “Research and development of innovative technologies for nuclear reactor core material with enhanced safety (2) High temperature steam oxidation and water corrosion characteristics of silicon carbide for reactor core,” *Proc. 2016 Spring Meeting of the Atomic Energy Society of Japan*, Sendai, March 26-28, 2016, 1H02, the Atomic Energy Society of Japan, (2016).
- [9] M. UCHIHASHI, M. UKAI, S. SUYAMA, K. KAKIUCHI, T. TAKAGI, and A. KAWAGUCHI, “Progress on ATF Development of SiC for LWR –Improvement of Corrosion Resistance–,” *Proc. 2017 Spring Meeting of the Atomic Energy Society of Japan*, Hiratsuka, March 27-29, 2017, 2J16, Atomic Energy Society of Japan, (2017).
- [10] X. HU, C. K. ANG, G. P. SINGH, and Y. KATOH, “Technique Development for Modulus, Microcracking, Hermeticity, and Coating Evaluation Capability for Characterization of SiC/SiC Tubes,” ORNL/TM-2016/372, (2016).
- [11] C. K. ANG, K. A. TERRANI, J. BURNS, and Y. KATOH, Examination of Hybrid Metal Coatings for Mitigation of Fission Product Release and Corrosion Protection of LWR SiC/SiC, ORNL/TM-2016/332, (2016).
- [12] R. ISHIBASHI, S. TANABE, T. KONDO, S. YAMASHITA, and F. NAGASE, “Improving the Corrosion Resistance of Silicon Carbide for Fuel in BWR Environments by Using a Metal Coating,” *Proc. WRFPM 2017*, Jeju Island, Korea, September 10-14, 2017, paper No.A-177_F-177, Korean Nuclear Society (2017).
- [13] T. KOYANAGI, Y. KATOH, G. SINGH, and M. SNEAD, SiC/SiC Cladding Materials Properties Handbook, Nuclear Technology Research and Development, ORNL/TM-2017/385, (2017).
- [14] K. ISHIDA, Y. WADA, M. TACHIBANA, N. OHTA, and M. FUSE, “Effects of Flow Rate on Dissolution of Monocrystal Alumina and Monocrystal Yttria-Stabilized Zirconia in High-Temperature Pure Water,” *Journal of Nuclear Science and Technology*, **46**, 1120-1128, (2009).
- [15] D. A. CRERAR and G. M. ANDERSON, “Solubility and Solvation Reactions of Quartz in Dilute Hydrothermal Solutions,” *Chemical Geology*, **8**, 107–122 (1971).
- [16] R. ISHIBASHI, K. ISHIDA, K. MIYAZAKI, and T. KONDO, “Development of Corrosion Resistant Coating Technology to Silicon Carbide Fuel Materials (2),” *Proc. 2018 Spring Meeting of the Atomic Energy Society of Japan*, Osaka, March 26-28, 2018, 3D10, Atomic Energy Society of Japan, (2018).